Synopsis of technical report

OPTI 521
Masaki Hosoda
Due Nov. 2, 2009

Paper:
Design of quasi-kinematic couplings
Martin L. Culpepper
Precision Engineering 28 (2004) 338-357

Abstract
A quasi-kinematic coupling (QKC) can be used as a fixing device with low-cost and sub-micron precision, instead of kinematic couplings. QKC consist of arc contacts formed by mating three balls with three axisymmetric grooves. Since a QKC is not an exact constraint, a proper design is required for producing a weakly over constrained coupling which emulates an exact constraint coupling. In this paper, practical design of QKC, derivation for predicting QKC stiffness, and experimental results showing repeatability is equal to 1/4 um are covered.
This study is sponsored by Ford Motor Company, but anybody, such as photonics, optical and other general company or institution can use this technique. Applications of this technique can be spread over a wide field, such as an automotive engine, optical mount, and other field requiring high precision.

1. Introduction

The quasi-kinematic coupling (QKC) is expected as a low-cost and sub-micron coupling. The traditional couplings, such as pinned joint, tapers, dove-tails and rail-slots, are not compatible with this condition. A kinematic coupling can provide better than 1 um precision alignment repeatedly. But it does not satisfy the low-cost requirement, because grooves with fine surface finish are expensive, high-hardness balls and grooves are desired to withstand Hertzian contact stresses, and kinematic couplings need additional flexures for sealing interfaces.

2. Quasi-kinematic coupling concept

In the case of kinematic coupling, the balls and grooves form small-area contacts. On the other hand, in the case of QKC, the balls and grooves form arc contact. This is the fundamental difference between kinematic coupling and QKC. Since QKC uses symmetric geometries, it is easier to manufacture.

Figure 4 (left) shows that, for the case of kinematic coupling, there are constraints between the balls and grooves in directions normal to the bisectors of the coupling triangle. There is freedom of motion in directions parallel to the bisectors. On the other hand, Figure 4 (right) shows that, for the case of QKC, there are constraint perpendicular to the bisector and some constraint along the bisectors. Then, QKC has some degree of over constraint.

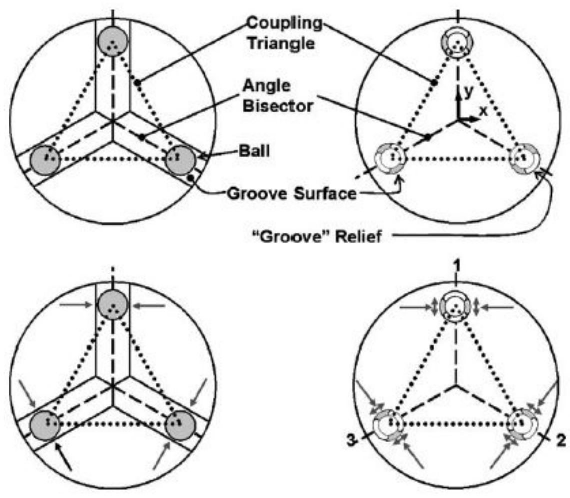

Fig. 4. Planar constraints in kinematic (left) and quasi-kinematic (right) couplings.

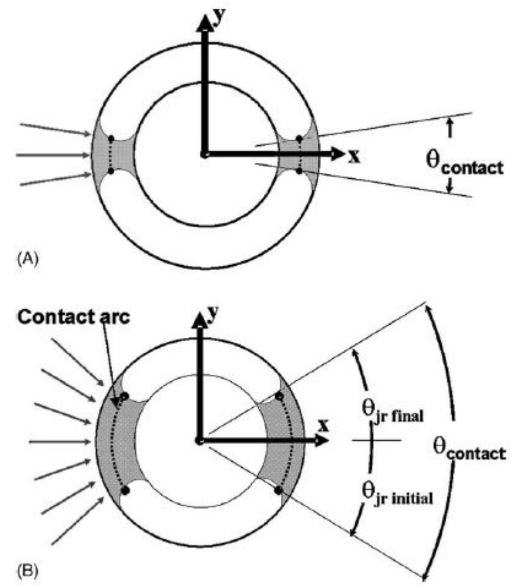

Fig. 5. The link between $\theta_{contact}$ and over constraint in QKCs with (A) small $\theta_{contact}$ and (B) large $\theta_{contact}$.

Figure 5 shows that the relationship between the contact angle and constraint contributions that are parallel to the y direction. The constraint contributions can be reduced by making the contact angle smaller, but this also reduces coupling stiffness. QKC has stiffness-constraint trade-off. This trade-off is discussed in section 3.

QKC meets the requirement for Low-cost generation of fine surface finish. By applying sufficient mating force and sliding tangentially between balls and surfaces of grooves, QKC balls can burnish surfaces of the grooves. For this purpose, the balls should be polished and have Young's modulus three to four times that of grooves. Second, QKC meets the requirement for Low-cost generation of alignment feature shape, because grooves are axisymmetric. Third, QKC also meets the requirement for Low-cost means to add Z compliance by using a hollow core shown in Figure 7. By increasing a nesting force and unloading the force, the ball-groove joints suffer plastically deform and elastic recovery. Then Z compliance can be obtained.

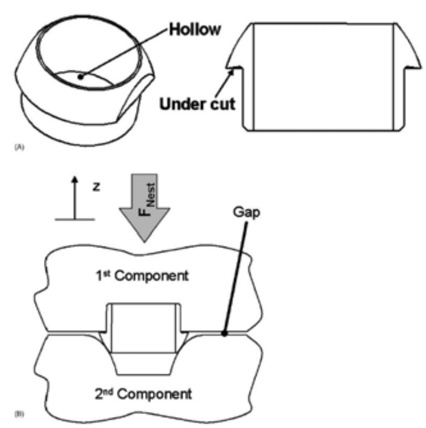

Fig. 7. Geometry of (A) compliant quasi-kinematic ball and (B) cross-section of a QKC joint.

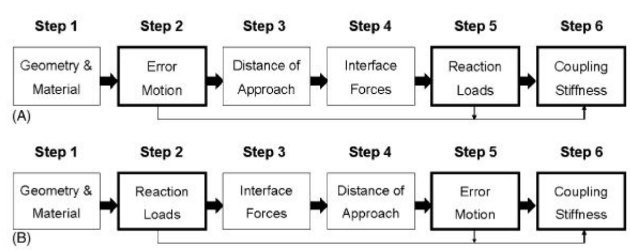

Fig. 8. Stiffness modeling strategies for (A) quasi-kinematic and (B) kinematic couplings.

3. Theory of quasi-kinematic couplings

The difference between analyzing kinematic coupling and QKC is shown in Figure 8. For analyzing QKC model, each step is shown briefly in the following.

Step 1: material and geometry characteristics

Figure 13 and Figure 14 show geometry characteristics.

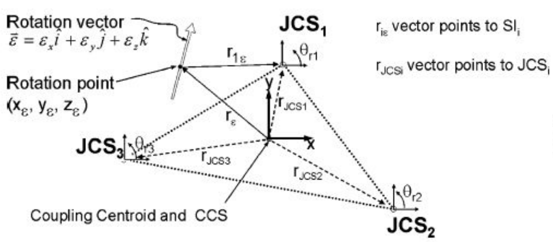

Fig. 13. Geometry characteristics of QKCs.

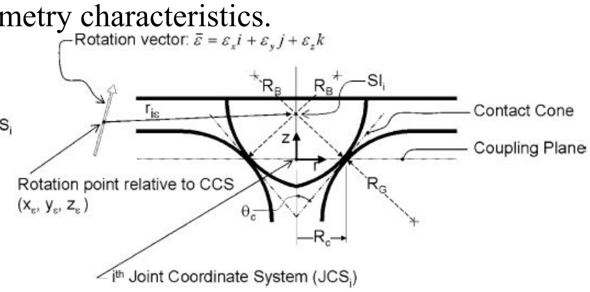

Fig. 14. Geometry characteristics of quasi-kinematic coupling joints.

Step 2: imposed error motions

Figure 15 shows displacement characteristics.

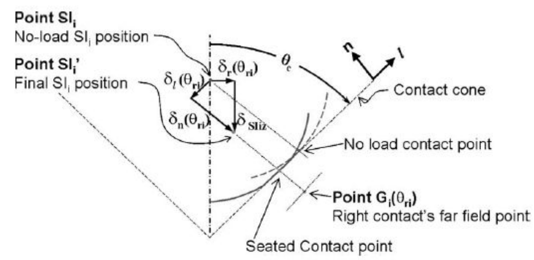

Fig. 15. Positions and motions of ball and groove far field points.

Step 3: distance of approach

The axial and radial displacements, and displacement perpendicular to contact cone are defined by the following equations (A.2) and (A.3).

$$\begin{bmatrix} \delta_r(\theta_{ri}) & \hat{r} \\ \delta_{SI_iz} & \hat{k} \end{bmatrix} = \begin{bmatrix} (\delta_{SI_ix}^2 + \delta_{SI_iy}^2)^{0.5}\cos[\theta_{ri} - \mathrm{atan}(\delta_{SI_iy}/\delta_{SI_ix})] & \hat{r} \\ \delta_{SI_iz} & \hat{k} \end{bmatrix} \tag{A.2}$$

$$\vec{\delta}_n(\theta_{ri}) = \left\{ -(\delta_{SI_ix}^2 + \delta_{SI_iy}^2)^{0.5} \cos phantom\left(\frac{\delta_{SI_iy}}{\delta_{SI_ix}}\right) \left[\theta_{ri} - \mathrm{atan}\left(\frac{\delta_{SI_iy}}{\delta_{SI_ix}}\right)\right]\cos(\theta_c) + \delta_{SI_iz}\sin(\theta_c) \right\}\hat{n} \tag{A.3}$$

Step 4: modeling interface forces

The force per unit length of contact $f_n(\theta_{ri})$ can be calculated with contact deformation in combination with integral compliance. The relationship between $f_n(\theta_{ri})$ and $\delta_n(\theta_{ri})$ is defined by

$$\vec{f}_n(\theta_{ri}) = K[\delta_n(\theta_{ri})]^b\hat{n} \tag{A.4}$$

where K is a stiffness constant and b is a rate of change in contact stiffness with changing $\delta_n(\theta_{ri})$.

Step 5: reaction force on an arc contact

By Figure 17., the reaction force at a contact arc j is defined by

$$\vec{F}_j = \int_{s_{\text{initial}}}^{s_{\text{final}}} [f_n(\theta_{ri})\hat{n}(\theta_{ri}) + f_l(\theta_{ri})\hat{l}(\theta_{ri}) + f_s(\theta_{ri})\hat{s}(\theta_{ri})]\,\mathrm{d}s \approx \int_{\theta_{jr\,\text{initial}}}^{\theta_{jr\,\text{final}}} [f_n(\theta_r)\hat{n}(\theta_{ri})]R_c\,\mathrm{d}\theta_{ri} \tag{A.5}$$

When a rotation matrix is considered for each vector i, j, k, the total reaction force is defined by

$$\vec{F}_j = \begin{bmatrix} \int_{\theta_{jr\,\mathrm{initial}}}^{\theta_{jr\,\mathrm{final}}} \{R_c\, K(\delta_n(\theta_{ri}))^b[-\cos(\theta_{ri})\cos(\theta_c)]\,\mathrm{d}\theta_{ri}\} & \hat{i} \\ \int_{\theta_{jr\,\mathrm{initial}}}^{\theta_{jr\,\mathrm{final}}} \{R_c\, K(\delta_n(\theta_{ri}))^b[-\sin(\theta_{ri})\cos(\theta_c)]\,\mathrm{d}\theta_{ri}\} & \hat{j} \\ \int_{\theta_{jr\,\mathrm{initial}}}^{\theta_{jr\,\mathrm{final}}} \{R_c\, K(\delta_n(\theta_{ri}))^b[\sin(\theta_c)]\,\mathrm{d}\theta_{ri}\} & \hat{k} \end{bmatrix}$$

Step 6: stiffness calculation

The coupling stiffness in the direction of the error displacement is calculated by

$$k_{\mathrm{imposed}} = \frac{\mathrm{d(Reaction)}}{\mathrm{d(Imposed\ error\ displacement)}} \qquad \mathrm{(A.11)}$$

Next, over constraint in QKC is considered. An over constraint is evaluated by the constraint metric (QM) defined by

$$\mathrm{CM}_i = \frac{\text{Stiffness parallel to bisector}}{\text{Stiffness perpendicular to bisector}} = \frac{k_{i\ \|\mathrm{Bisector}}}{k_{i\ \perp\mathrm{Bisector}}} \qquad (1)$$

When the relieved groove joint design described by Figure 9A and Table 1 is considered, the joint's radial stiffness plot in Figure 9B can be obtained by the above theory. The relationship between $\theta_{contact}$ and CM or the maximum radial stiffness K_{max} is described in Figure 10. By this figure, the better condition of CM and K_{max} can be chosen for a specification.

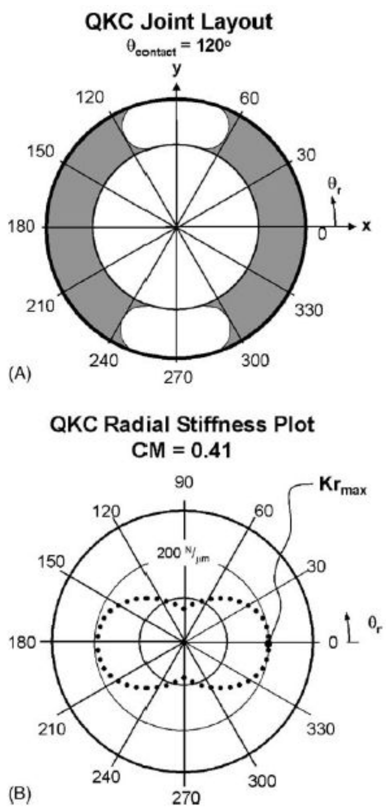

Fig. 9. Example QKC relieved groove (A) orientation and (B) stiffness for $\theta_c = 45°$; $\theta_{contact} = 120°$; $K\,(\mathrm{N/\mu m^{2.07}}) = 1 \times 10^{-2}$; $b = 1.07$; $R_c = 0.66$ cm; $\delta_{z\text{-preload}} = -60\ \mu$m.

Table 1
Example QKC joint design characteristics

Design variable	Value
R_c	0.66 cm (0.260 in.)
$\delta_{z\text{-preload}}$	−60 µm (−0.002 in.)
K	1×10^{-2} (N/µm$^{2.07}$) (2948850(lb/in.$^{2.07}$))
b	1.07
$\theta_{contact}$	120°
θ_c	45°

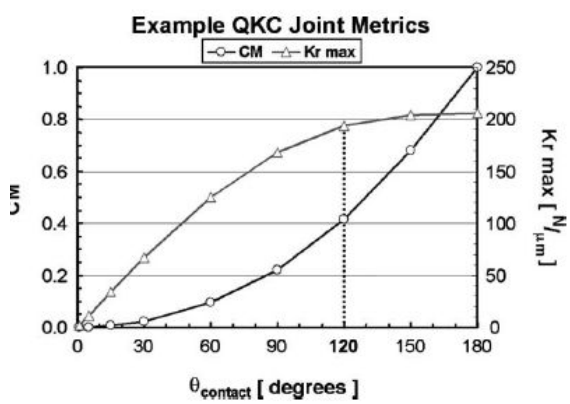

Fig. 10. Comparing performance metrics of QKCs.

4. Testing the MathCAD model

When the MathCAD tests a model that would make the ball loose contact with the groove, the model detects this as a violation.

5. Experimental result

The experimental setup and repeatability results are shown in Figure 11. $\theta_{contact}$ is set to 60 deg., then CM is 0.10 in this case. The result shows the coupling repeats in-plane to 1/4 um after an initial wear-in period.

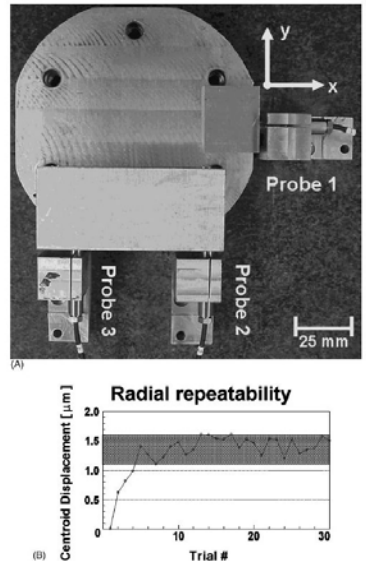

Fig. 11. QKC (A) test setup and (B) repeatability results for $\theta_c = 32°$; $\theta_{contact} = 60°$; K (N/μm$^{2.07}$) $= 1 \times 10^{-2}$; $b = 1.07$; $R_c = 0.66$ cm; 25 N preload.

6. Coupling cost

The ball-groove sets would cost about $1 for greater than 100,000 couplings per year, or about $60 for less than several hundred per year.

7. Conclusion

This paper provides the theory and metric that can minimize the degree of over constraint in QKC. Experimental result shows that QKC can provide precision alignment (1/4 um) that is comparable to kinematic couplings. Subsequent research will study an alignment errors caused by mismatch between ball and groove patterns.

8. Reference

M. Barraja, R. Vallance, “Tolerancing kinematic couplings,” Precision Engineering 29 , 101–112 (2005)